2nd year contractor report for:
U.S. Department of Energy
Stewardship Science Academic Alliances Program

Sponsor ID #: **DE-FG03-02NA00060**
TEES (Texas A&M) Project#: **69390/32525**

Project Title:
Detailed Measurements of Rayleigh-Taylor Mixing at Large and Small Atwood Numbers

Report date: December 14, 2004
Project starting date: September 14, 2002
Principle Investigator: Professor Malcolm J. Andrews
Department of Mechanical Engineering
Texas A&M University, College Station, TX 77845
Tel: (979) 847 8843 or (409) 847 8843
e-mail: mandrews@mengr.tamu.edu

Abstract

This project has two major tasks:

- Task 1. The construction of a new air/helium facility to collect detailed measurements of Rayleigh-Taylor (RT) mixing at high Atwood number, and the distribution of these data to LLNL, LANL, and Alliance members for code validation and design purposes.
- Task 2. The collection of initial condition data from the new Air/Helium facility, for use with validation of RT simulation codes at LLNL and LANL. Also, studies of multi-layer mixing with the existing water channel facility.

Over the last twelve (12) months there has been excellent progress, detailed in this report, with both tasks. As of December 10, 2004, the air/helium facility is now complete and extensive testing and validation of diagnostics has been performed. Currently experiments with air/helium up to Atwood numbers of 0.25 (the maximum is 0.75, but the highest Reynolds numbers are at 0.25) are being performed. The progress matches the project plan, as does the budget, and we expect this to continue for 2005. With interest expressed from LLNL we have continued with initial condition studies using the water channel. This work has also progressed well, with one of the graduate Research Assistants (Mr. Nick Mueschke) visiting LLNL the past two summers to work with Dr. O. Schilling. Several journal papers are in preparation that describe the work. Two MSc.'s have been completed (Mr. Nick Mueschke, and Mr. Wayne Kraft, 12/1/03). Nick and Wayne are both pursuing Ph.D.s' funded by this DOE Alliances project. Presently three (3) Ph.D. graduate Research Assistants are supported on the project, and two (2) undergraduate Research Assistants. During the year two (2) journal papers and two (2) conference papers have been published, ten (10) presentations made at conferences, and three (3) invited presentations.

Contents

1. RESULTS AND ACCOMPLISHMENTS

1.1 Introduction

The project involves collecting statistical turbulence data from a new high Atwood (At) number Rayleigh-Taylor (R-T) mixing facility that has been built as part of the project. The experiment investigates buoyancy driven R-T mixing that is relevant to ICF implosion. The data has been, and will continue to be, provided to Alliance members (specifically LLNL and LANL) for code validation and turbulence model formulation/testing. The experiment is a natural follow-on from our small Atwood number (water channel) facility that has been in use for almost 10 years. The new facility has now been built and uses *air and helium* to achieve Atwood numbers up to 0.75. Since mixing of air and helium is involved the fluids are miscible with Prandtl and Schmidt numbers close to one. The new air/helium facility is similar to the water channel whose details may be found in the papers associated with the present work, referenced in section 6 below, and included on the CD associated with this report. The water channel is a statistically stationary R-T experiment that allows long data collection times (10 minutes or greater in the water channel, and up to 2 minutes in the new gas channel). The long data collection times have allowed us to obtain sufficient data for a spectral analysis of the R-T mixing process. The new air/helium facility is intended to provide similar statistical data but for high Atwood number R-T mixing.

The organization of this second year progress report is to present a description of the accomplishments and results, and in particular progress and results from the new air/helium gas channel, and initial condition studies performed with the water channel. This is followed by a schedule of work for the final year, and the current project personnel. The report closes with an account of alliance activities, purchases, publications and presentations from the project, financial status, and an appendix with additional details about the air/helium facility.

1.2 Task 1: Construction of the new Air/Helium RT Mix Facility

This task spans the first and second years of the project, and is associated with the construction and shakedown of the new air/helium facility.

Figure 1 (over the page) shows a schematic of the air/helium facility taken from the proposal. Figure 2 shows a photograph of the new air/helium facility (as of August, 2004), with Mr. Michael Peart (undergraduate Research Assistant) as a reference scale. Inspection of figure 2 shows that construction of the facility is complete and corresponds to the schematic design. However, one significant improvement has been made, the depth of the flow channel has been increased from 60 cm to 120 cm (4ft), the width from 40 cm to 60 cm (2ft), and the length from 3 m to 6 m (19ft). This change was done to increase the operational Reynolds number by a factor of two (2), so it will now approach 20,000, with a nominal increase in cost, and no need for additional funds. The flow channel dominates the center of the photograph, and may be divided into four parts going from right to left; the entrance duct work that feeds air on top and helium below (the helium bottles are behind the flow channel and not visible in the photograph); the splitter plate that starts with the honeycomb flow straightener and continues with wire meshes to control boundary layer development; after the splitter comes the main flow channel where buoyancy driven mixing takes place; and lastly, the exit plenum that vents to the outside. Below the flow channel can be seen air intakes for fans that feed the channel.

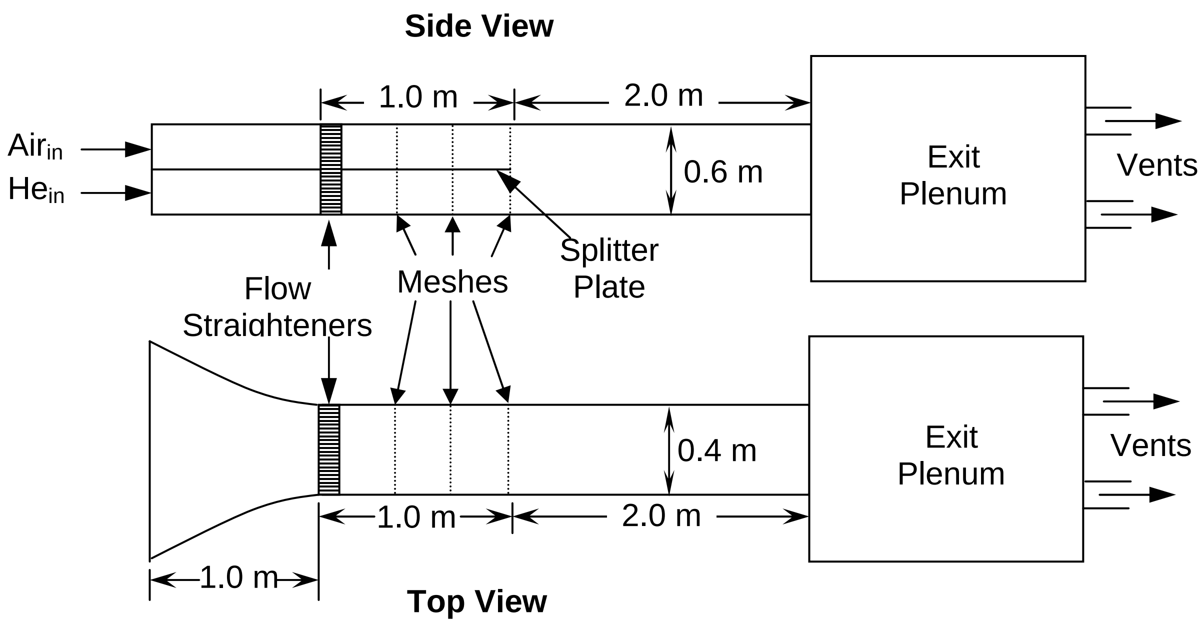

Figure 1. Schematic of the Air/Helium Facility taken from the Proposal

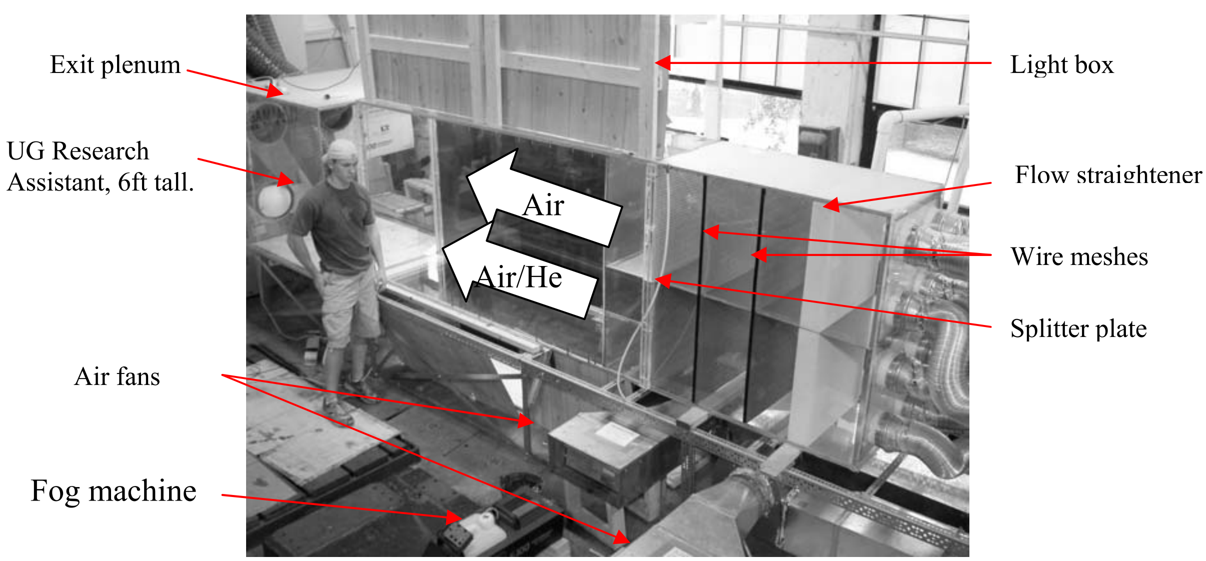

Figure 2. Photograph of Gas Channel, August 2004.

1.3 Task 1 cont.: Calibration and Results from the Air/Helium Facility

Over the past year we have made good progress with the Air/Helium channel. The major elements of the work have involved three significant tasks described in the following subsections.

1.3.1 Obtaining a constant mass flow rate of helium from the supply bottles:

A key component for the successful operation of the facility is to supply a known and constant mass flow rate of Helium from the supply bottles. With such a careful control, we choose the Atwood number by then mixing helium with a known mass flow rate of air. Indeed, obtaining a constant mass flow rate of helium was a troublesome problem (the mixing with air was readily achieved with impingement plates in the flow channel). Our solution is fully described in Appendix A, where we show that our arrangement of orifices and regulators provides the necessary constant mass flow rate. Moreover, the use of two regulators in series, has allowed us to extract approximately 90% of the available helium from a bottle, while maintaining a constant mass flow rate. The system is now arranged so we can run pure helium, at a known constant mass flow rate, through the mixing channel to give Atwood numbers up to 0.75. Having completed a system with a constant mass flow rate of helium, we have now moved on to calibration of the diagnostics and obtaining results for Atwood numbers up to 0.21.

1.3.2 Calibration and validation of the hot wire system for velocity measurements:

Our planned primary diagnostic is a hot wire system for accurate measurements of velocity from which we can obtain Reynolds stresses, and by way of a thermocouple, mean density profiles and density fluctuations. The hot wire system was purchased from Dantec at the end of 2003 (see last year's scientific report). This year we have calibrated the system for Atwood numbers up to 0.25, and have collected data for Atwood number of 0.035 for comparison/validation with results from the water channel. A detailed discussion of the hot wire calibration is given in Appendix B, and the next section presents a selection of our results for Atwood numbers up to 0.21.

1.3.3 Measurements for RT mixing up to an Atwood number of 0.21:

Table 1 and Figure 3 are taken from Appendix B, and contain velocity measurements taken from the air/helium and water channels. Data collected at At=0.035 from the air/helium channel is presented so we might compare the measurements with those from our well established water channel that operates up to At=0.001. Table 3 presents horizontal (u' and w) and vertical (v') RMS velocity fluctuation measurements. The anisotropy of these measurements (v'/u') is close to that measured in the water channel, and reported by the PI in Ramaprabhu and Andrews (2004), and referenced in section 6.1.1. In addition the value for the self-similar growth parameter, α, is also consistent at about 0.07. Indeed, Figure 3 plots the collapse of α against distance downstream (equivalent to time from Taylors' hypothesis) for the water channel (from Ramaprabhu and Andrews, 2004) and the measured values from the air/helium channel, the agreement is excellent. Thus, we have concluded that the hot wire diagnostics are performing well, and that the gas channel can be operated in a manner that faithfully reproduces the successful performance of the water channel.

x (m)	u'	v'	w'	$u'/\overline{u}$	$v'/\overline{u}$	v'/u'	$\alpha = \frac{v'}{2A_t gt}$	$T = \frac{x}{U}\left(\frac{A_t g}{H}\right)^{\frac{1}{2}}$
1.0	0.0879	0.1051	0.0729	0.1353	0.1617	1.1951	0.1004	0.8126
1.75	0.0724	0.1286	0.1009	0.1114	0.1978	1.7747	0.0702	1.4220
1.95	0.0837	0.1440	0.0753	0.1287	0.2216	1.7218	0.0706	1.5845

Table 1. Hot wire velocities (m/s) at Atwood # 0.035 ($\overline{u}$ = 0.60 m/s).

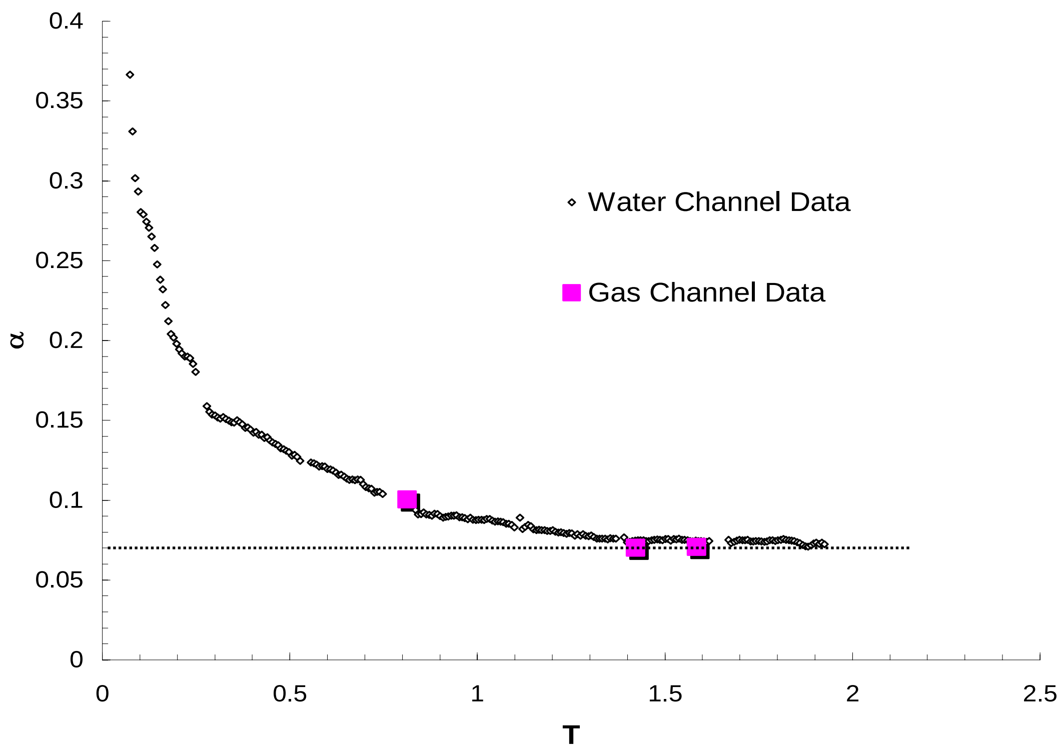

Figure 3. Comparison of the alpha growth rate parameter measured from the water channel (At=7.5e-4) and the new He/Air facility (At=0.035).

To illustrate the performance of the gas channel at higher Atwood numbers Figures 5A to 5C are photographs taken a Atwood numbers that correspond to 0.035, 0.097, and 0.21. To ensure the flow remains parabolic, and thus Taylors' hypothesis is applicable, the speed of the gas stream is increased from 0.6 m/s to 1.45 m/s. The photographs show that this increase in mean axial gas velocity keeps the required small spread angle, and corresponds to the design guidelines for the facility that were given in the original proposal. Thus, we have found no surprises about the required gas flow rates, and this indicates we will be able to run the facility at the highest At of 0.75 at an expected cost of around $100 to $300 per run. The similarity of the gas channel photographs (5A to 5C) and the water channel (5D) also supports our statement that, at these practically symmetric mix Atwood numbers, the two experiments are closely similar. At the highest Atwood number of 0.75 we can expect to see asymmetry around the centerline of the mix, and this will be one of the focus areas in the next year (see section 2 below).

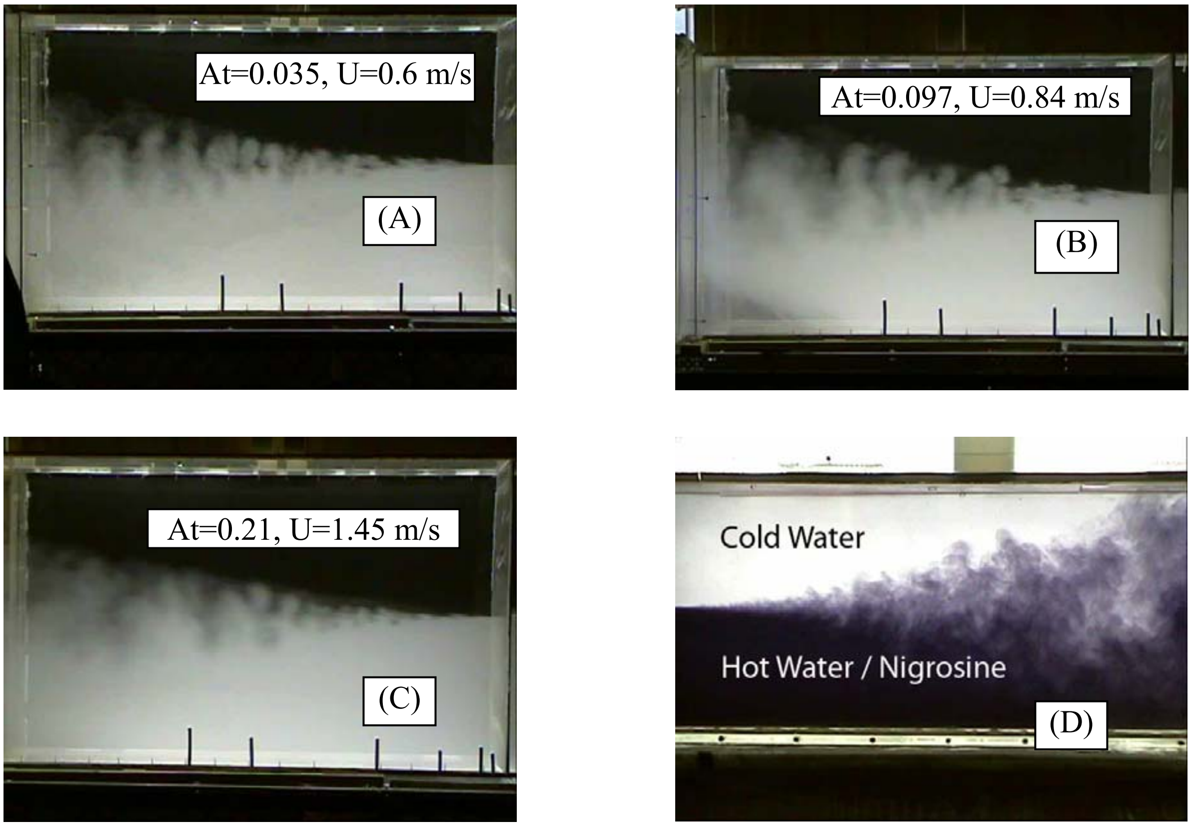

Figure 4. Photographs from the He/Air gas channel (A) through (C), and the water channel (D) (note the fluid streams run the opposite way in the water channel).

1.3.4 Summary of progress with the air/helium mixing channel

Progress has been excellent with the main construction now finished, and the successful completion of shakedown tests. Our results for small Atwood number correspond well to the water channel. Plans for the coming year are described in section 2.

1.4 Task 2: Collection of Initial Condition Data

This task involves a new set of experimental measurements for initial conditions in our R-T mixing experiments. These experimental initial conditions are then used to start corresponding DNS computer simulations of the R-T mixing process.

In the proposal this task was scheduled to begin in 2004, however, interest from LLNL and the availability of a graduate research assistant led us to start this task early using the water channel facility. This work has continued during 2004, as we continue our Alliances with LLNL and LANL, with data being transferred to Dr. Oleg Schilling at LLNL.

1.4.1 Experimental work completed

Experimental measurements have been taken in the water channel facility to quantify initial density and velocity fluctuations in an incompressible, miscible, small Atwood number Rayleigh-Taylor mixing layer. Density and velocity fluctuations have been measured with high-resolution thermocouples and particle image velocimetry, respectively. The density fluctuations were then transformed to an interfacial perturbation spectrum. In the last year several *new* experiments were performed to measure the two-fluid interfacial perturbation in the *spanwise* direction using planar laser-induced fluorescence (PLIF). The data acquired just off the splitter plate was then parameterized to obtain initial conditions for use in numerical simulations at LLNL.

Two new sets of measurements have been made that comprise initial velocity conditions and initial density interfacial perturbations in the spanwise direction.

Figure 5 shows a schematic of the camera and laser sheet arrangement used to measure the cross stream interfacial perturbations. An image correction algorithm (2^{nd} order-polynomial dewarping algorithm) was used to correct the images so that quantitative data could be extracted. Results from these measurements produced a spectrum of interfacial density perturbations, that have been applied to initial perturbations for a DNS simulation of the water channel (details described in the next sub-section).

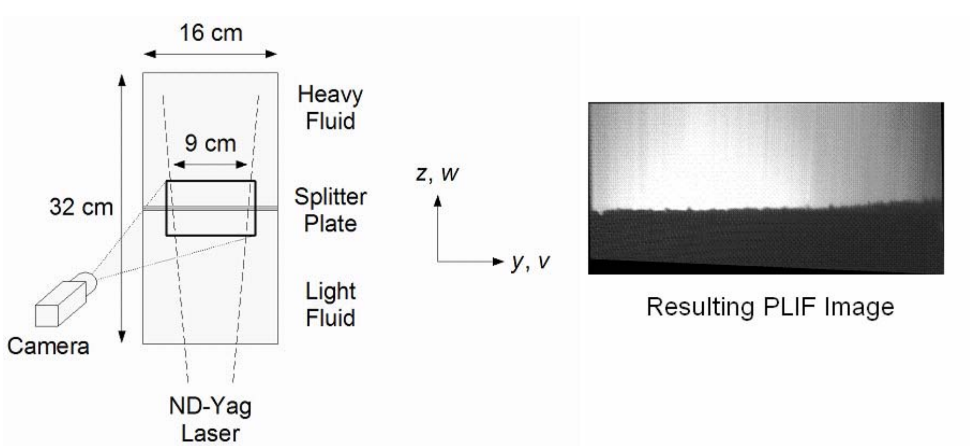

Figure 5. Schematic of Cross-Stream PLIF measurement and example photograph.

1.4.2 Computational work completed

Three-dimensional direct numerical simulations (DNS) of the Texas A&M water channel Rayleigh-Taylor mixing experiment have been performed at LLNL with Dr. Oleg Schilling. The simulations at LLNL used the spectral/compact difference code MIRANDA, with simulation parameters chosen to match the densities, viscosities, diffusivities, and physical dimensions in the experiment. These DNS simulations were seeded with either initial density perturbations, or with initial density and velocity perturbations. Experimentally measured statistical quantities were compared with those obtained from DNS, including integral-scale, small-scale, and turbulence statistics. A key conclusion from comparison between DNS and experiment was that initial velocity perturbations are required to adequately match experimental data, rather than just density fluctuations. Further details may be found in the APS presentations given in 6.2.1 and 6.2.2 below, and given on the associated CD. This work is presently being written-up into an experimental paper for submission to Physics of Fluids, and afterwards a theoretical/computational paper for the Journal of Fluid Mechanics.

Figure 6 below illustrates a comparison between experiment and DNS simulation, where computed temperature profiles and PLIF photographs are shown: (a) PLIF from the water channel at $x \approx 35$ cm; and, (b) 3D DNS (256×128×256). The comparison is not quite one-to-one because the PLIF marker and temperature do not coincide perfectly (the temperature diffuses faster). However, the sizes and general shapes are comparable and indicate very encouraging agreement.

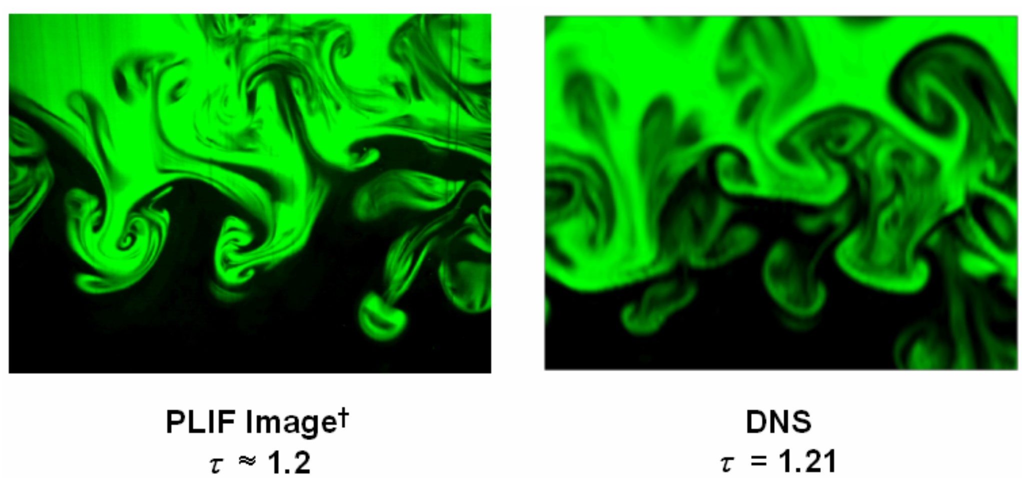

Figure 6. Comparison of experimental PLIF image with corresponding DNS simulation.

1.5 Summary of Significant Achievements and Progress in the 2nd Year

- The new air/helium R-T mixing facility has been constructed, and tests performed that show a very satisfactory performance for Atwood numbers up to 0.25.

- Initial condition research has indicated that use of initial velocity fluctuations better represents the initial conditions in the experiment, and that high resolution simulations are needed to resolve short wavelength disturbances in the initial conditions of the experiment.
- Arranging for a constant mass flow rate of Helium from the supply bottles proved to be a troublesome task. However, after some work we implemented a successful design (given in Appendix A) that provides a constant mass flow rate, and has been carefully calibrated.
- The hot wire diagnostic has been calibrated and successfully used to collect statistical data.

1.6 Summary of Completed Project Tasks for Years 1 & 2

All tasks from year 1 have been completed.

Tasks from Proposal

Task 1: Completed: Construction of Air/Helium Facility		
Task 1.1	Familiarization of post-doc and student A (prepare drawings, obtain materials, order hot-wire equipment)	Done
Task 1.2	Construct facility (build channel and familiarization with hot-wire	Done
Task 1.3	Preliminary validation and shakedown tests	Done
Task 2: Data collection from the Air/Helium Channel		
Task 2.1	Preliminary validation (small and high Atwood number testing). Continue with initial condition testing in water channel.	Completed
Task 2.2	Obtain measurements for mix width, $\overline{u'^2}$, $\overline{v'^2}$, $\overline{u'v'}$, and $\overline{\rho'^2}$.	30% done
Task 3: Initial Condition studies		
Task 3.A	Initial condition studies using the Air/Helium channel - preliminary studies in the water channel	50% done

2. PROJECT SCHEDULE FOR YEAR 3

This third year of the project will see us concentrate on collecting high quality data from high Atwood number experiments (At=0.75), and explore the highest Reynolds number condition that occurs around At=0.25. We will also continue and complete the initial condition studies. The proposal also included three layer studies – if time permits we will address this task, however in the event that the task is not completed we anticipate that the work will be continued as part of a follow-on proposal.

Year 3 Tasks from Proposal: Experiments in the Air/Helium Facility

Task 2.2	Obtain measurements for mix width, $\overline{u'^2}$, $\overline{v'^2}$, $\overline{u'v'}$, and $\overline{\rho'^2}$ at Atwood numbers up to 0.75 .	To be completed
Task 3A	Initial condition studies using the Air/Helium channel - preliminary studies in the water channel.	To be completed
Task 3B	Three-layer mix experiments – if time permits.	To be completed

In addition to these tasks from the proposal we also plan to continue with publications and conference presentations, with prior submission to DOE and NNSA for approval.

3. PARTICIPANTS AT TAMU DURING THE 2ND YEAR

PI:	Dr. Malcolm J. Andrews: US Citizen
Graduate Research Assistants:	Mr. Michael Martin (Ph.D.): US Citizen
	Mr. Arindam Banerjee (Ph.D.): India Citizen
	Mr. Nicholas Mueschke (MSc./Ph.D.): US Citizen
	Mr. Wayne Kraft (MSc./Ph.D.): US Citizen
Undergraduate Research Assistants:	Ms. Amanda Dellaughter: US Citizen
	Mr. Michael Peart: US Citizen

4. ALLIANCE EXCHANGE ACTIVITIES

- Nicholas Mueschke spent the summer (03 and 04) as a LLNL graduate researcher working with Dr. Oleg Schilling. The outcome of this work has been described above.

- Dr. Praveen Ramaprabhu completed his Ph.D. and has started (12/8/2003) work at Los Alamos.

- Mr. Wayne Kraft spent one week during the summer of 2004 at LANL (it was to be July and August, but the the lab went through a shutdown and so Wayne returned to continue his research at TAMU).

- The PI visited with LLNL and LANL collaborators throughout the year either at conferences or on the phone.

- Dr. Oleg Schilling visited Texas A&M University in October 2004, and reviewed the gas channel facility with Dr. David Youngs.

It is our pleasure to host Alliance collaborators to the water channel and gas channel facilities, and we are pleased to run the experiments, and involve colleagues in the research.

5. PURCHASES

There has been no major single purchase this year. However, we continue to purchase materials (e.g. Helium, smoke fluid), miscellaneous diagnostic items (e.g. wire, connectors, probes), and continue with minor improvements to the facilities (e.g. the light box shown in figure 2).

6. PUBLICATIONS AND PRESENTATIONS REFERENCING PROJECT (see CD for copies)

6.1 Publications

6.1.1 Ramaprabhu, P., and Andrews, M.J., "Experimental Investigation of Rayleigh-Taylor Mixing at Small Atwood Numbers," *Journal of Fluid Mechanics*, Vol. 502, pp. 233-271, March, 2004.

6.1.2 Ramaprabhu, P., and Andrews, M.J., “On the Initialization of Rayleigh-Taylor Simulations," *Physics of Fluids* A, Vol. 16, No. 8, pp. L59-L62, August 2004.

6.1.3 Kraft, N.W., and Andrews, M.J., “Experimental Investigation of Stratified, Buoyant Wakes” Paper # HT-FED2004-56623, 2004 ASME Heat Transfer/Fluids Engineering Summer Conference Westin Charlotte & Convention Center Charlotte, North Carolina, USA July 11-15, 2004**,** Proceedings: ISBN: 0-7918-3740-8.

6.1.4 Mueschke, N., and Andrews, M.J., “Investigation of Scalar Measurement Error in Diffusion and Mixing Processes” Paper IMECE2004-60993, 2004 ASME International Mechanical Engineering Congress & Exposition, Anaheim, California, USA, Nov. 13-19, 2004**,** Proceedings: ISBN: 0-7918-4178-2.

6.1.5 Mueschke, N.J., “An Investigation of the Influence of Initial Conditions on Rayleigh-Taylor Mixing,” MSc. Thesis, Texas A&M University, Dec. 2004.

6.1.6 Kraft, W., “Experimental Investigation of a Stratified Buoyant Wake,” MSc. Thesis, Texas A&M University, Aug. 2004.

6.2 Conference Presentations Since Last Report

6.2.1 Mueschke, N., Schilling, O., and Andrews, M.J., “Measurement of Initial Conditions of a ayleigh-Taylor Mixing Layer” DFD2004, Bulletin of the American Physical Society, Vol. 49, No.9, p. 223, November, 2004.

6.2.2 Mueschke, N., Schilling, O., and Andrews, M.J., “Direct Numerical Simulations of Rayleigh-Taylor Mixiing with Experimentally Measured Initial Conditions” DFD2004, Bulletin of the American Physical Society, Vol. 49, No.9, p. 223, November, 2004.

6.2.3 Kraft, N.W., and Andrews, M.J., “A Stratified Buoyant Wake” DFD2004, Bulletin of the American Physical Society, Vol. 49, No.9, p. 224, November, 2004.

6.2.4 Banerjee, A., and Andrews, M.J., “Progress with a High Atwood Number Statistically Steady Rayleigh-Taylor Mix Experiment” DFD2004, Bulletin of the American Physical Society, Vol. 49, No.9, p. 222, November, 2004.

6.2.5 Kraft, N.W., and Andrews, M.J., “Experimental Investigation of Stratified, Buoyant Wakes” Paper # HT-FED2004-56623, 2004 ASME Heat Transfer/Fluids Engineering Summer Conference Westin Charlotte & Convention Center Charlotte, North Carolina, USA July 11-15, 2004**,** Proceedings: ISBN: 0-7918-3740-8.

6.2.6 Mueschke, N., and Andrews, M.J., “Investigation of Scalar Measurement Error in Diffusion and Mixing Processes” Paper IMECE2004-60993, 2004 ASME International Mechanical Engineering Congress & Exposition, Anaheim, California, USA, Nov. 13-19, 2004**,** Proceedings: ISBN: 0-7918-4178-2.

6.2.7 Kraft, W.N., and Andrews, M.J., "Visualization of Rayleigh-Taylor Instability," poster, 9th International Workshop on the Physics of Compressible Turbulent Mixing, Cambridge, UK, 19-23, July, 2004.

6.2.8 Ramaprabhu, P., and Andrews, M.J., "An Overview of Rayleigh-Taylor experiments at Texas A&M University," poster, 9th International Workshop on the Physics of Compressible Turbulent Mixing, Cambridge, UK, 19-23, July, 2004.

6.2.9 Dimonte, G., Ramaprabhu, P., and Andrews, M.J., "Dependence of Self-Similar Rayleigh-Taylor Growth on Initial Conditions," presentation, 9th International Workshop on the Physics of Compressible Turbulent Mixing, Cambridge, UK, 19-23, July, 2004.

6.2.10 Schilling, O., Mueschke, N., and Andrews, M.J., "Direct Numerical Simulations of Miscible, Small Atwood Number Rayleigh-Taylor Instability-Induced Mixing," presentation, 9th International Workshop on the Physics of Compressible Turbulent Mixing, Cambridge, UK, 19-23, July, 2004.

6.3 Other Presentations

6.3.1 Andrews, M.J., "Turbulent Mixing by Buoyancy Driven Rayleigh-Taylor Instability," Department of Mechanical Engineering, Clemson University, Clemson, South Carolina, February 20, 2004.

6.3.2 Mueschke, N., Schilling, O., Andrews, M.J., "Experimentally-based initialization of direct numerical simulations of miscible, Rayleigh-Taylor instability-induced mixing," presentation given to Complex Hydrodynamics Group, LLNL, August 12, 2004.

6.3.3 Andrews, M.J., "Progress with Turbulent Mixing by Buoyancy Driven Rayleigh-Taylor Instability," Stewardship Science Academic Alliances (SSAA) Program Symposium, Albuquerque, New Mexico, March 29 – 31, 2004.

7. FINANCIAL STATUS (as of December 2004)

Please see next page for details. The project is keeping to budget.

The % time supported is as follows:

Position	Person	Time
PI	Dr. Malcolm J. Andrews	15%
Graduate Research Assistant	Mr. Wayne Kraft	50%
Graduate Research Assistant	Mr. Arindam Banerjee	50%
Graduate Research Assistant	Nicholas Mueschke	50%
Undergraduate Research Assistant	Ms. Amanda Dellaughter	~20%
Undergraduate Research Assistant	Mr. Michael Peart	~20%

8. APPENDIX: Details of the Air/Helium Facility

8.1 Appendix A: Formulation and Calibration of Constant Mass Flow Rate

The velocities of the two streams are set in such a manner that there is no shear between the flows ($U_{air} = U_{mixture} = U_m$). Since the cross sectional area (A) of the top and bottom sections are identical, the volumetric flow rate of air and helium- air mixture in the top and bottom channels respectively are equal. The flow rate of mixture in the bottom section of the channel is then given by:

$$\dot{V}_{mixture} = \dot{V}_{air} + \dot{V}_{Helium} = \dot{V}_{air} + \frac{\dot{m}_{Helium}}{\rho_{Helium}} = U_m A \quad (A.3)$$

The density of the air-Helium mixture is calculated based on the Gibb's Dalton Law as:

$$\rho_{mixture} = \rho_{air}(1-X) + \rho_{He}X = \rho_{air}\frac{\dot{V}_{air}}{\dot{V}_{mixture}} + \rho_{He}\frac{\dot{V}_{Helium}}{\dot{V}_{mixture}} \quad (A.4)$$

where X is the volume fraction of Helium in the mixture. Substituting Equation (A.3) in (A.4) and simplifying, we get:

$$\rho_{mixture} = \rho_{air} + \frac{\dot{m}_{He}}{U_m A}\left[1 - \frac{\rho_{air}}{\rho_{Helium}}\right] \quad (A.5)$$

The only unknown parameter in Equation (A.5) is the mass flow rate of Helium ($\dot{m}_{He}$). The objective is thus to calibrate the flow rate using the method described below. Once the density of mixture is known, the Atwood Number of the mix is known accurately as follows:

$$A_t = \frac{(\rho_1 - \rho_2)}{(\rho_1 + \rho_2)} = \frac{(\rho_{air} - \rho_{mixture})}{(\rho_{air} + \rho_{mixture})} = \frac{\left[\frac{\rho_{air}}{\rho_{mixture}} - 1\right]\frac{\dot{m}_{Helium}}{U_m A}}{2\rho_{air} + \left[1 - \frac{\rho_{air}}{\rho_{mixture}}\right]\frac{\dot{m}_{Helium}}{U_m A}} \quad (A.6)$$

<u>Estimation of Mass Flow Rate ($\dot{m}_{He}$) of Helium:</u>

Since the mass flow rate of helium ($\dot{m}_{He}$) must be precisely known to evaluate the Atwood Number, an accurate estimation of the flow rate is required. Initial consideration was given to using a commercial gas flow meter or controller. However for the range of pressures (~ 2000 psig) and mass-flow rates being used (~0.1 lbm/s), the flow meters are expensive. Furthermore, calibration data obtained from the manufacturers were based on air and using empirical laws to compensate for the effects of Helium meant that the device required re-calibration. Thus it was decide to use a volumetric method at constant outlet pressure for flow metering. In this method, the gas delivered from a supply passes through a flow constriction, preferably an orifice, and is delivered to its final destination (Berman, 1985). Jitschin et al (1995) uses a similar method to accurately measure gas flows by using a combination of a pressure gauge, an orifice and a vernier leak valve to measure the flow rate. Similarly, the main feature of the flow-meter used with the current set-up is the use of a thin orifice for flow constriction and metering. The pressure drop across the orifice is maintained such that the pressure ratio between the downstream and upstream locations is below the critical pressure ratio. The flow is choked at the orifice and thus the mass flow rate through it can be determined based on empirical relations. However, when using an orifice for flow constriction, the coefficient of discharge (C_d) must be evaluated. Therefore, the mass flow rate was measured by placing the helium bottle(s) on a sensitive digital read-out and recording the change in weight of the bottle with time. The uncertainty of the digital scale is ± 0.01 lbs. The mass flow rate obtained by this method was compared with the theoretical calculations and a coefficient of discharge was calculated for the range of orifices used.

Figure A1 is a schematic of the setup being used for metering the mass flow rate of Helium into the gas channel. Two high pressure regulators R1 and R2 (TESCOM, Inc.) are used to control the pressure drop from a supply pressure of ~ 2000 psig to the ambient pressure inside the channel where the unit vents the Helium. Two high pressure gauges (Swagelock, Inc.) are connected as shown in the schematic to accurately read the pressure in the line at two different downstream locations. ¼" steel tubing is used to connect all the components. An orifice plate is placed after the downstream pressure gauge and held in position by the flow control valve. Initially, the flow control valve is closed and the pressure regulators are adjusted. The upstream regulator is fixed at 1050 psig which ensures that the pressure ratio across R1 exceeds the critical pressure ratio and thus the flow is not choked at R1. Similarly, maintaining the downstream pressure

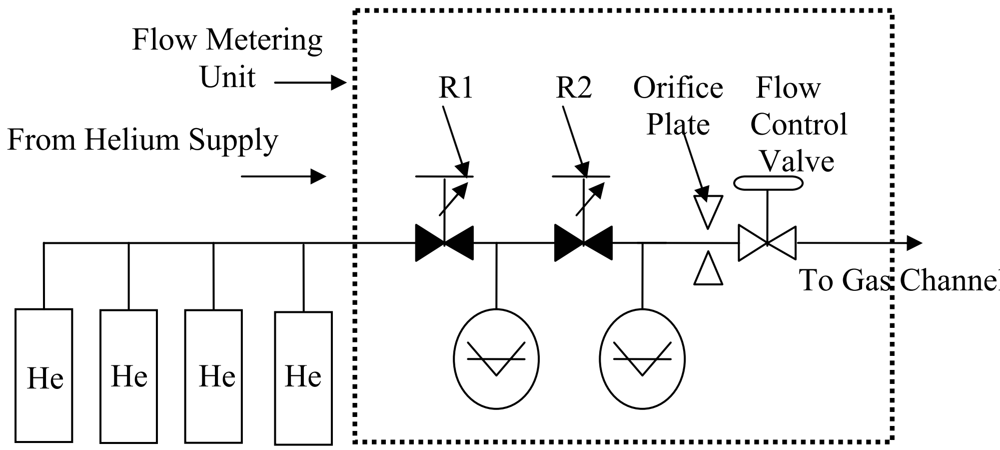

Figure A1. Experimental Setup for metering Helium mass flow rate

regulator R2 at 550 psig ensures that the flow is not choked at R2. Thus as soon as the flow control valve is opened, the flow is immediately choked at the orifice which ensures a constant mass flow rate of Helium until the pressure in the bottles drops below the set pressure (550 psig in this case).

Table A1 shows the results of the mass flow rate calibration and the coefficient of discharge (C_d) for three different orifices of diameters 0.032", 0.061" and 0.11". The theoretical mass flow rate is calculated based on equations for sub-critical flow through the orifice. The mass flow rate was measured by placing the helium bottle(s) on a sensitive digital read-out and recording the change in weight of the bottle with time. The uncertainty of the digital scale is ± 0.01 lbs. Figures A3 (a) to (c) illustrates the mass flow rates of Helium measured with three different orifices. A straight line fit is performed through the data points obtained and the mass flow rates are tabulated. The R^2 values for the fit in these cases vary between 0.9992 and 0.9998. The discharge coefficient (C_d) is seen to vary between 0.87 and 0.91 for the range of orifice used. The Atwood number range tabulated below is calculated based on the experimental mass flow rate and varying the angle of spread in the mix between 10º - 15º.

Diameter of Orifice (inch)	Mass Flow Rate (lbm/s)		$C_d = \dot{m}_{\exp} / \dot{m}_{theory}$	Atwood Number
	Experimental	Theory		
0.032	0.0066	0.0072	0.9166	0.035-0.042
0.061	0.0234	0.0267	0.8764	0.082-0.100
0.110	0.0796	0.0869	0.9159	0.194-0.259

Table A1. Calibrated Mass flow rates for different Orifice

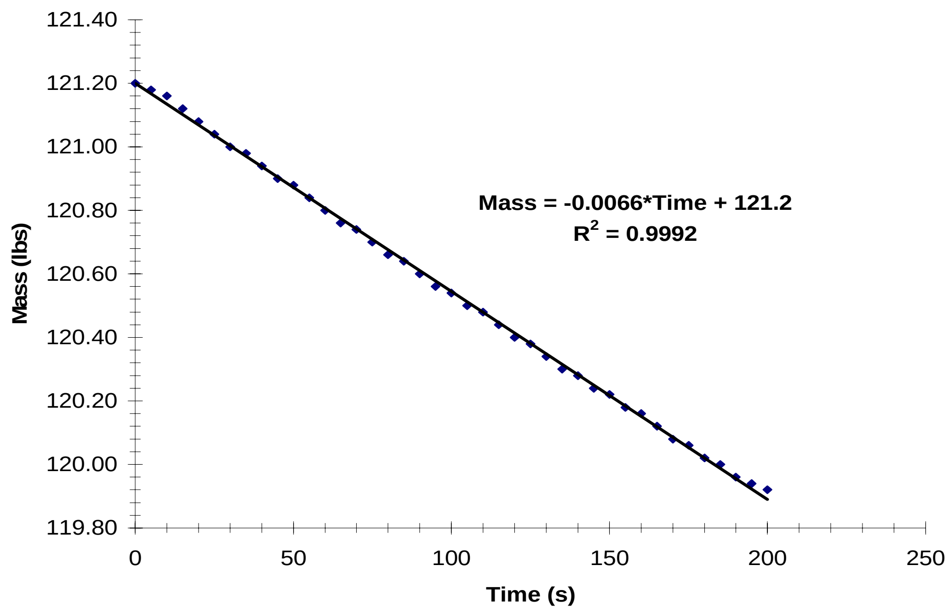

Figure A3a. Calibration Run for orifice diameter 0.032 inch

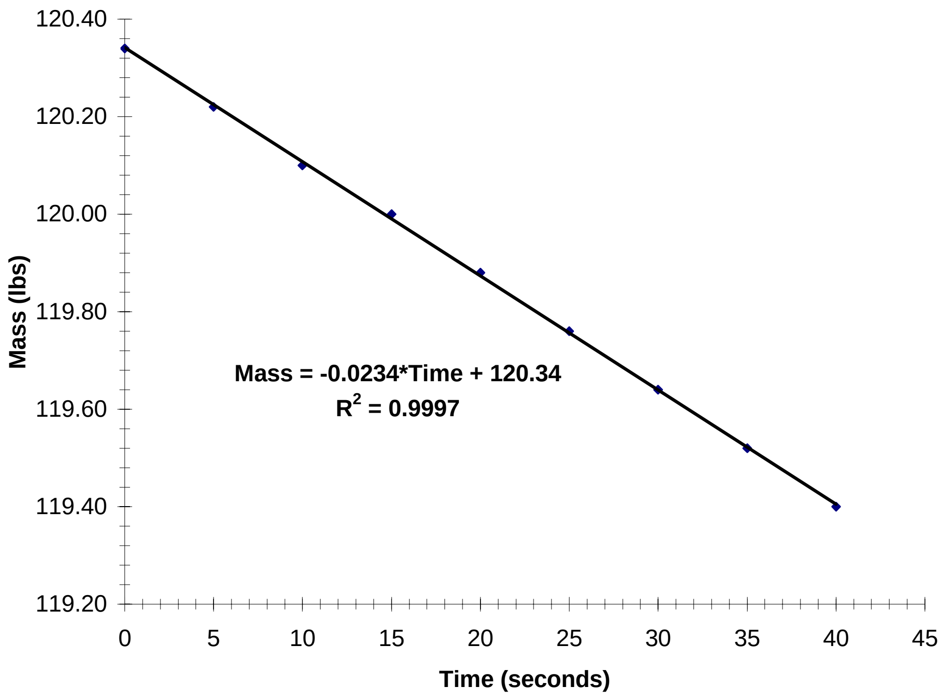

Figure A3b. Calibration Run for orifice diameter 0.061 inch

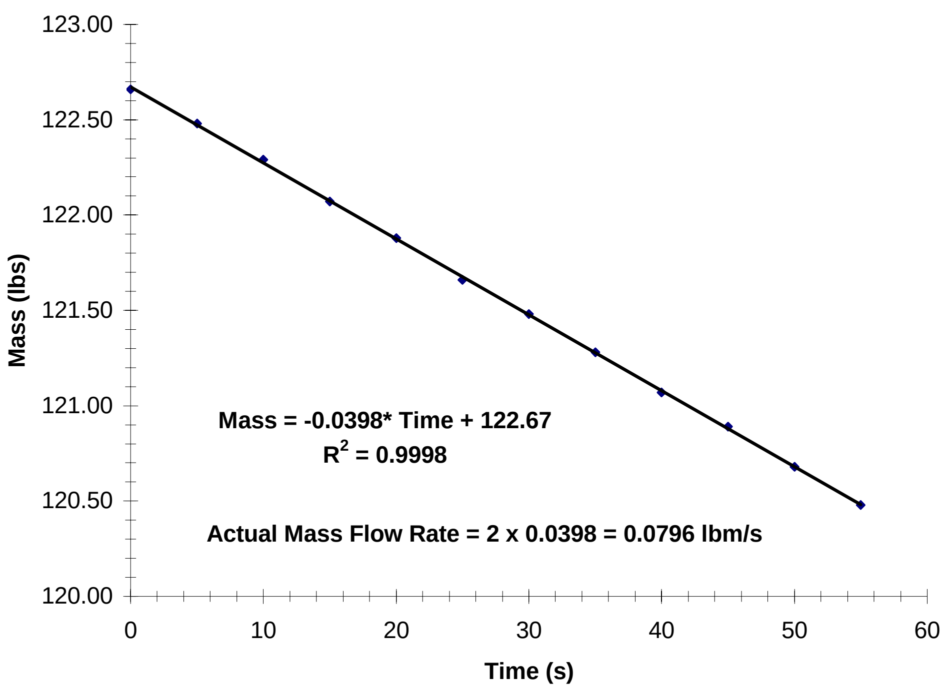

Figure A3c. Calibration Run for orifice diameter 0.110 inch

References:

- Berman, A. *Total Pressure Measurements in Vacuum Technology*, Academic Press, Orlando, FL (1985).
- Jitschin, W., Weber, U., and Hartmann, H.K., Convenient primary gas flow meter, *Vacuum*, Vol. 46, No 8-10, pp. 821-824 (1995).

8.2 Appendix B: Appendix: Measurement Technique with Constant Temperature Anemometer (CTA)

The Constant Temperature Anemometer (CTA) is an analog instrument designed for measuring velocity in gases, and is particularly suited for measurement of fast gas velocity fluctuations. It works on the basis of convective heat transfer from a heated sensor to the surrounding fluid, the heat transfer being primarily related to the fluid velocity. By using fine wire sensors placed in the fluid and electronics with a servo-loop technique, it is possible to measure velocity fluctuations of fine scales and high frequencies. The advantages of the CTA over other flow measuring principles are ease of use, analogue voltage output (which means that no information is lost), and very high temporal resolution, which makes the CTA ideal for measuring spectra.

System Configuration

A CTA unit (54T30) was purchased from Dantec Dynamics. The device is mounted in a small box equipped with BNC connectors and operated from a 12 VDC power adapter. The bandwidth (max. 10 kHz) is optimized for use with wire probes. The anemometer accepts probes with cold resistances up to 10 Ω. The complete measuring system consists of the following:

- Single Normal Hot-wire probe (SN probe: Model # 55P16) with support and 4-m BNC-BNC probe cable.
- The Mini-CTA anemometer with built-in signal conditioner and power adapter.
- Output BNC-BNC cable.
- SC 2040 Sample and Hold Board (National Instruments) with flat cable to A/D board.
- A PCI-MIO-16E-4 A/D board (National Instruments) mounted in a PC.
- NI-DAQ driver software, Mini-CTA application software and Lab-View DAQ Software.

The principle of the CT circuit is illustrated in Figure B1. The hot wire probe is placed in a Wheatstone bridge. As the flow conditions vary, the error voltage $e_2 - e_1$ will be a measure of the corresponding change in the wire resistance. These two voltages form the input to the operational servo amplifier. The selected amplifier has an output current, *i*, which is inversely proportional to the resistance change of the hot wire sensor. Feeding this current back to the top of the bridge will restore the sensor's resistance to its original value.

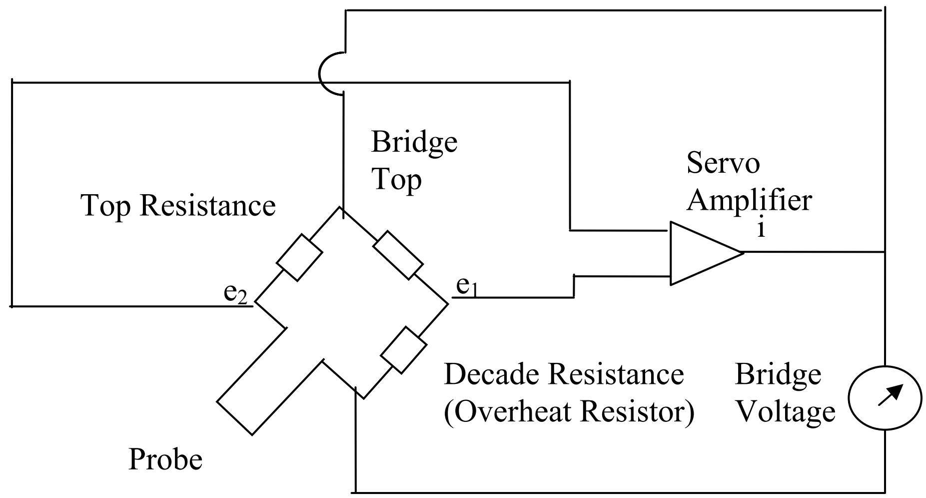

Figure B1. The CT Anemometer contains a Wheatstone bridge and a feedback amplifier.

Modern amplifiers have a very fast response time. Furthermore, in the CT mode, the sensor can be maintained at a constant temperature except for very high frequency fluctuations. The 54T30 Mini CTA circuit operates on bridge ratio of 1:20 and has a frequency response of 10 kHz (3 dB limit). The various CTA and probe parameters are listed in Table B1. A 55P16 single normal probe is used for the present measurements. The various parameters tabulated below correspond to specifications for the SN probe as provided by the manufacturer (Dantec Dynamics).

Insert probe specific parameters etc.		
Sensor resistance, R_{20}	3.30	Ω
Sensor lead resist., R_L	0.50	Ω
Support resistance, R_s	0.40	Ω
Cable resistance, R_c	0.20	Ω
Sensor TCR, α_{20}	0.36%	/K
Desired wire temp., T_w	187	°C
Temperature of flow	20	°C
Calculating wire operating resistance etc.		
Over temperature, ΔT	167	°C
Operating resistance, R_w	5.28	Ω
Total resistance, R_T	6.38	Ω
Overheat ratio, a	0.60	
Bridge ratio, M	1:20	
Decade resistance, R_D	127.7	Ω

Table B1. Operating Parameters for Mini-CTA

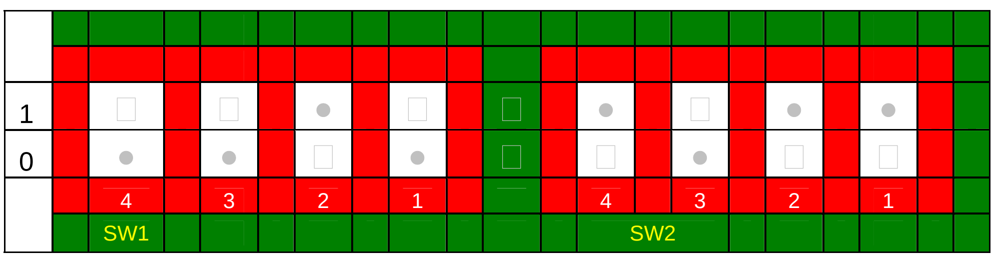

Figure B2. Decade switch adjustments to control overheat ration for Mini-CTA

CTA Adjustment

The overheat adjustment determines the working temperature of the sensor. The overheat resistor (decade resistor) in the right bridge arm, as illustrated in Figure B1, is adjusted so that the desired sensor operating temperature is established when the bridge is set to operate. The Mini-CTA software calculates the decade setting on the basis of the sensor resistance entered during set-up. The overheat adjustment may be based on either the wire resistance at 20ºC as stated on the probe container or the measured wire resistance at the actual temperature. Overheat setup and signal conditioning is done by dip switches and jumpers inside the box as illustrated in Figure B2. A grey dot in the calculated pattern indicates that this side of the dip switch is pressed down. The decade resistance is set according to the pattern displayed in Figure B2 which is obtained from the Mini-CTA software.

Velocity Calibration

Calibration establishes a relation between the CTA output and the flow velocity by exposing the probe to a set of known velocities, *U*, and then recording the voltages, *E*. A curve fit through the points *(E,U)* represents the transfer function to be used when converting data records from voltages into velocities. Calibration may either be carried out in a dedicated probe calibrator or in a wind tunnel with for example a pitot-static tube as the velocity reference. Temperature is recorded during calibration. If it varies from calibration to measurement, the CTA data records are corrected for temperature variations using Equation (B1).

$$E_{corr} = \left(\frac{T_w - T_0}{T_w - T_a} \right)^{0.5} \cdot E_a \qquad \text{(B1)}$$

Calibration of the S-N Wire probe (55P16) performed over a velocity range of 0 – 1.8 m/s as illustrated in Figure B3 (a). A 4th order polynomial plot is fitted to this data and it is found to have a R^2 value of 0.998. The errors associated with the 4th order polynomial fit can be attributed to the measurement of velocity in the gas channel. The errors associated with the 4th order fit in Fig. B3 (a) can be attributed to errors in velocity measurement inside the gas channel. The maximum error for the range of calibration velocity is as low as 1.84%. Since a multi-position single sensor technique is used, it is essential to evaluate the yaw parameter *k* of the sensor. The calibration curve is illustrated in Figure B3 (b).

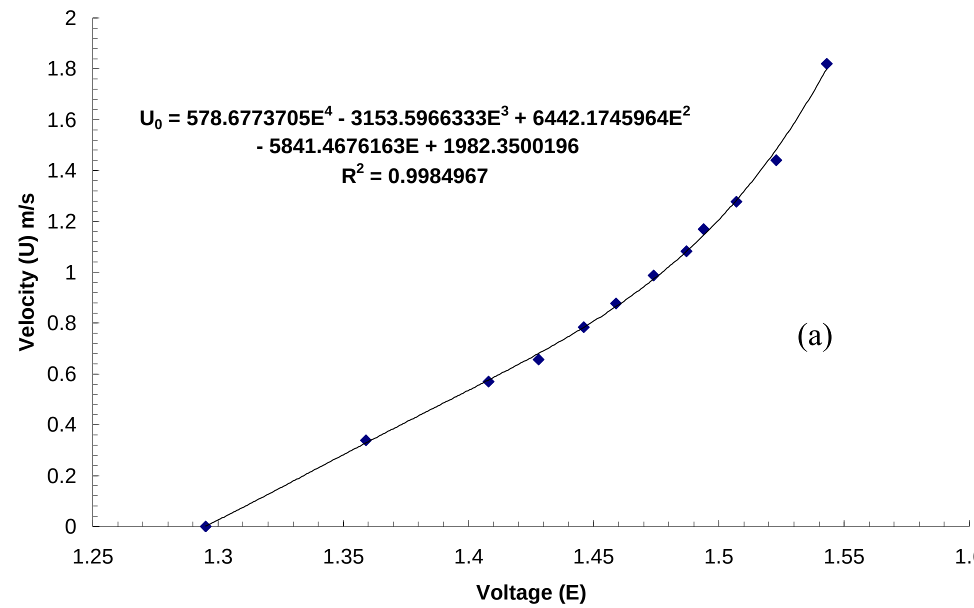

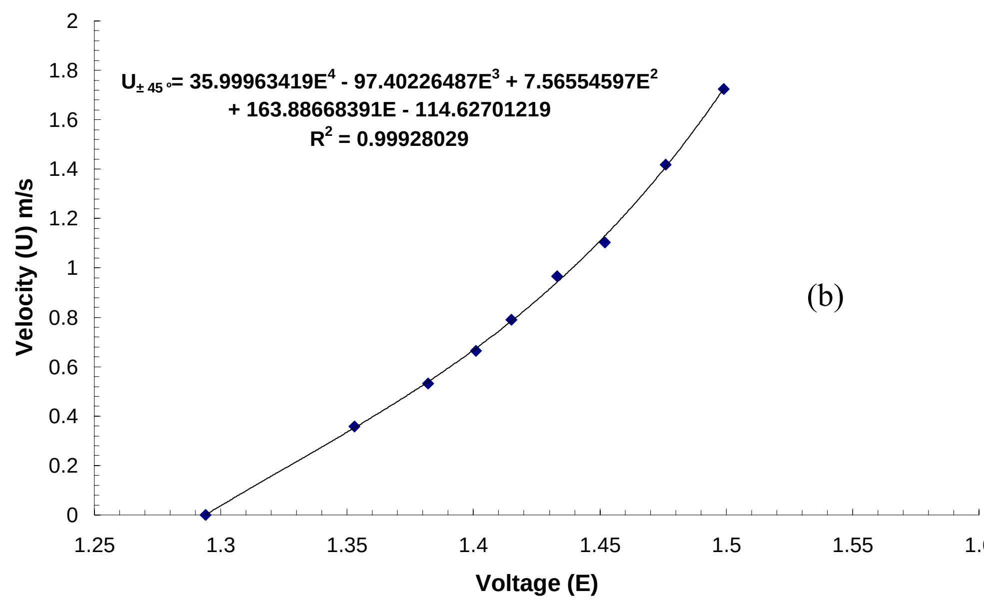

Figure B3b. Calibration curve of SN Hot wire (DANTEC 55P16) probe at Overheat Ratio (OR) of 0.6 in air at: (a) γ (yaw angle) = 0˚; (b) γ (yaw angle) = ± 45˚ to evaluate yaw coefficient *k*.

Measurement Methodology

For a RT mix experiment, velocity fluctuations in all 3 mutually perpendicular directions are significant. There are two alternatives to resolve the velocity fluctuations in the 3 directions:

1. Use a 3-wire probe to resolve all 3 components
2. Use a multi-position single - wire technique and then resolve the components from data reduction and analysis (Bruun ,1972).

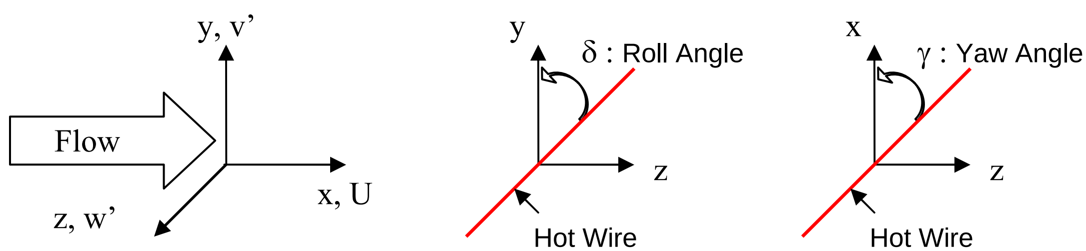

Figure B4. Co-ordinate System for measurements and Various Orientations of Hot Wire used for measurements (Probe axis is normal to the red line).

Position	γ	δ
1	0	0
2	45	90
3	-45	90

Table B2. Various measurement orientations for multi-position measurement technique

A multi-position single wire technique is being used for the current measurements as tabulated below. The velocity vector V is taken to have the velocity components $((\overline{U}+u', v', w')$.Individual measurements are made by changing the yaw angle of the probe axis as illustrated in Figure B4. The respective roll and yaw angles for the 3 different measurements are tabulated in Table B2. The series expansion for the instantaneous velocity $|\vec{V}|$ is derived in terms of the mean component velocity ($\overline{U}$), the mean velocity ratio ($\overline{V}/\overline{U}$) and the fluctuating components (u', v', w'). The relationship becomes, when maximum third order terms are included:

$$|\vec{V}| = \overline{U}\left[1 + \frac{1}{2}\frac{\overline{W}^2}{\overline{U}^2} + \frac{u}{\overline{U}} + \frac{\overline{W}}{\overline{U}}\frac{w}{\overline{U}} + \frac{1}{2}\frac{w^2}{\overline{U}^2} + \frac{1}{2}\frac{v^2}{\overline{U}^2} - \frac{\overline{W}}{\overline{U}}\frac{uw}{\overline{U}^2} - \frac{1}{2}\frac{uw^2}{\overline{U}^3} - \frac{1}{2}\frac{uv^2}{\overline{U}^3} + \frac{\overline{W}}{\overline{U}}\left(\frac{1}{2}\frac{u^2 w}{\overline{U}^3} - \frac{1}{2}\frac{w^3}{\overline{U}^3} - \frac{1}{2}\frac{v^2 w}{\overline{U}^3}\right)\right]$$

For $\overline{W} \approx 0$; $\frac{\overline{W}}{\overline{U}} << 1$, we get: $|\vec{V}| = \overline{U}\left[1 + \frac{u}{\overline{U}} + \frac{1}{2}\frac{v^2}{\overline{U}^2} + \frac{1}{2}\frac{w^2}{\overline{U}^2} - \frac{1}{2}\frac{uv^2}{\overline{U}^3} - \frac{1}{2}\frac{uw^2}{\overline{U}^3}\right]$ (B2)

Position 1: *Wire normal to mean flow direction and wire support parallel to flow*:

Mean Component: $$\overline{U}_m = \overline{U}\left[1 + \frac{1}{2}\frac{\overline{W}^2}{\overline{U}^2} + \frac{1+2b}{2}\frac{\overline{w^2}}{\overline{U}^2} - \frac{\overline{W}}{\overline{U}}\frac{\overline{uw}}{\overline{U}^2} - \frac{1+2b}{2}\frac{\overline{uw^2}}{\overline{U}^3}\right]$$

Since $\overline{W} \approx 0$ and ignoring 3rd order terms gives:

$$\overline{U}_m = \overline{U}\left[1 + \frac{1+2b}{2}\frac{\overline{w^2}}{\overline{U}^2}\right] \quad \text{(B3)}$$

For the fluctuating Component: $$\overline{u_m^2} = \overline{u^2}\left[1 + 2\frac{\overline{W}}{\overline{U}}\frac{\overline{uw}}{\overline{u^2}} + (1+2b)\frac{\overline{uw^2}}{\overline{u^2}\overline{U}} - (1+2b)\frac{\overline{u^2 w^2}}{\overline{u^2}\overline{U}^2}\right]$$

Since $\overline{W} \approx 0$ and ignoring 3rd and 4th order terms gives:

$$\overline{u_m^2} = \overline{u^2} \quad \text{(B4)}$$

Position 2: *Wire yawed to mean flow direction at an angle +γ :*

Mean Component:

$$\overline{U}_{+\gamma} = \overline{U}\{\cos^2\gamma + k^2 \sin^2\gamma\}^{\frac{1}{2}}\left[1 + \frac{1+2b+A\tan^2\gamma}{2}\frac{\overline{w^2}}{\overline{U}^2} - \frac{1+2b+A\tan^2\gamma}{2}\frac{\overline{uw^2}}{\overline{U}^3}\right]$$

Ignoring 3rd order terms gives:

$$\overline{U}_{+\gamma} = \overline{U}\{\cos^2\gamma + k^2 \sin^2\gamma\}^{\frac{1}{2}}\left[1 + \frac{1+2b+A\tan^2\gamma}{2}\frac{\overline{w^2}}{\overline{U}^2}\right] \quad \text{(B5)}$$

The fluctuating Component ignoring 3rd and 4th order terms can be written as:

$$\overline{u_{+\gamma}^2} = \{\cos^2\gamma + k^2 \sin^2\gamma\}\left(\overline{u^2} + A^2 \tan^2\gamma \cdot \overline{v^2} - 2A\tan\alpha \cdot \overline{uv}\right) \quad \text{(B6)}$$

Position 3: Wire yawed to mean flow direction at an angle -γ : For the fluctuating component (ignoring 3rd and 4th order terms) gives:

$$\overline{u_{-\gamma}^2} = \{\cos^2\gamma + k^2\sin^2\gamma\}\left(\overline{u^2} + A^2\tan^2\gamma\cdot\overline{v^2} + 2A\tan\alpha\cdot\overline{uv}\right) \qquad \text{(B7)}$$

Adding Equations (B6) and (B7), gives for $\overline{v^2}$:

$$\overline{v^2} = \frac{\overline{u_{+\gamma}^2} + \overline{u_{-\gamma}^2} - 2\{\cos^2\gamma + k^2\sin^2\gamma\}\overline{u^2}}{2\{\cos^2\gamma + k^2\sin^2\gamma\}A^2\tan^2\gamma}$$

Since $\gamma = 45°$:

$$\overline{v^2} = \frac{\overline{u_{+45}^2} + \overline{u_{-45}^2} - (1+k^2)\overline{u^2}}{(1+k^2)A^2} \qquad \text{(B8)}$$

Definition of parameters: *k*, *b* and *A* are constants associated with the yaw orientation of the probe and have been measured using standard techniques. For the yaw coefficient:

$$k = \frac{1}{\sin\alpha}\left[\left(\frac{E_{\alpha=45^\circ}^2 - E_{U=0}^2}{E_{\alpha=0^\circ}^2 - E_{U=0}^2}\right)^{\frac{2}{0.5}} - \cos^2\alpha\right]^{\frac{1}{2}} \qquad \text{(B9a)}$$

$$A = \frac{\cos^2\alpha\cdot(1-k^2)}{\cos^2\alpha\cdot(1-k^2)+k^2} = \frac{1-k^2}{1+k^2} \quad (\alpha = 45^\circ) \qquad \text{(B9b)}$$

$$V_e = V(1 + b\cdot\sin^2\alpha) \qquad \text{(B9c)}$$

Measurements were taken at 3 different locations (x = 1.0m, 1.75m and 1.95m) from the splitter plate. Care was taken to ensure that the hot wire was close to the center line of the mix. This was ensured with a thermocouple. The temperature diagnostics consisted of a vertical rake of thermocouples that were positioned at different downstream locations in the channel to ensure that the center line of the mix remains more or less horizontal. The thermocouple probe is E-type (nickel-chromium and constantan) and welded at the tip to form a bimetallic junction. The thermal response of the E-type thermocouple was ~0.001 s deg^{-1}, while the accuracy was ±0.13 deg. A 16-bit data acquisition board collected data from the thermocouples at a maximum sampling rate of 50,000 Hz. To remove some of the noise, local averages of over 500 samples are performed, resulting in a net sample rate of 100 Hz.

The centerline r.m.s. values of the vertical, *v'*, horizontal, *u'*, and cross wise, *w'*, at *T* locations of 0.8126, 1.422 and 1.5845 are tabulated below. The vertical velocity at the centerline can be related to the centerline of the mix width (Ramaprabhu and Andrews, 2004) by:

$$v' = \frac{dh}{dt} = 2\alpha A_t gt \quad \text{(B10)}$$

Equation B10 is valid only in the self similar region of the flow. Vertical velocity fluctuations dominate the horizontal and crosswise velocity fluctuations in this experiment with a ratio approaching 2:1 in the self similar region. From the time evolution of *v'*, we can determine the growth constant α by computing the ratio: $v'/2A_t gt$. This ratio is plotted as a function of non-dimensional time *T* in Figure B5. The results are compared with the Low Atwood experiments at the water channel facility performed earlier (Ramaprabhu and Andrews, 2004; Snider and Andrews, 1994). The comparison is illustrated in Figure B5.

x (m)	u'	v'	w'	$u'/\overline{u}$	$v'/\overline{u}$	v'/u'	$\alpha = \frac{v'}{2A_t gt}$	$T = \frac{x}{U}\left(\frac{A_t g}{H}\right)^{\frac{1}{2}}$
1.0	0.0879	0.1051	0.0729	0.1353	0.1617	1.1951	0.1004	0.8126
1.75	0.0724	0.1286	0.1009	0.1114	0.1978	1.7747	0.0702	1.4220
1.95	0.0837	0.1440	0.0753	0.1287	0.2216	1.7218	0.0706	1.5845

Table B3. Hot wire velocities (m/s) at Atwood # 0.03467 ($\overline{u}$ = 0.60 m/s).

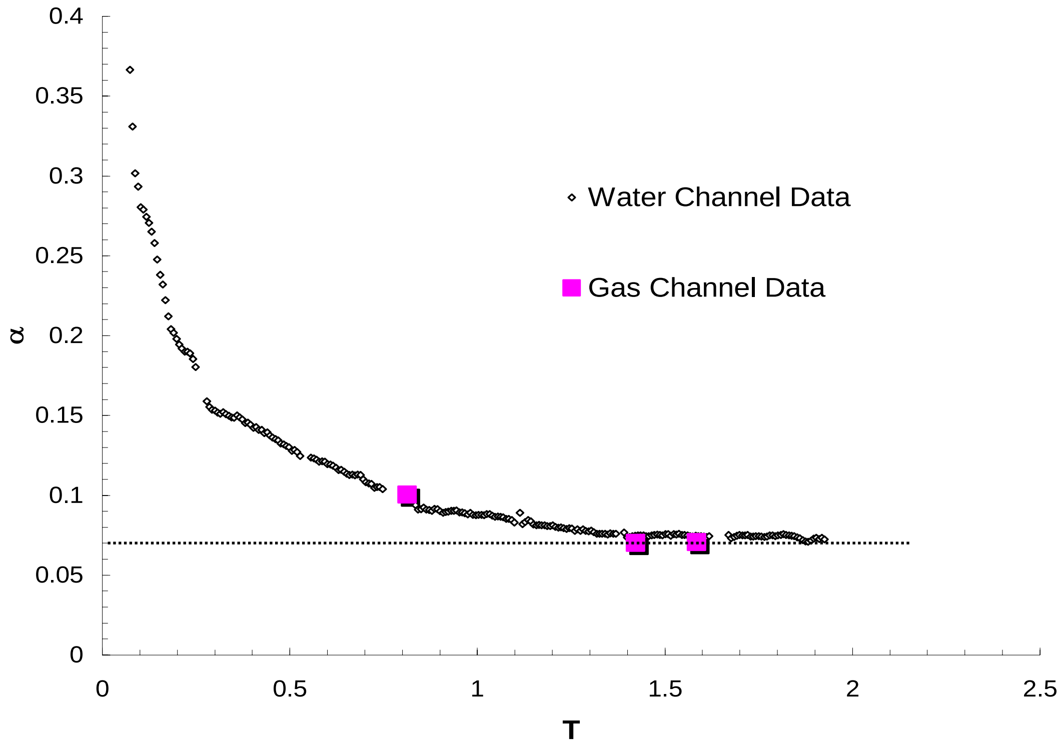

FigureB5. Comparison with Low Atwood Number (7.5 x 10^{-4} data from Water Channel Facility at Texas A&M University)

References:

- Bruun H.H. Hot-wire corrections in low and high turbulence intensity flows, *Journal of Physics E: Scientific Instruments*, Vol. 5, pp. 812-818 (1972).
- Ramaprabhu P. and Andrews M.J. Experimental investigation of Rayleigh- Taylor mixing at small Atwood numbers, *Journal of Fluid Mechanics*, Vol. 502, pp.233-271 (2004).
- Snider D.M. and Andrews M.J. Rayleigh-Taylor and shear driven mixing with an unstable thermal stratification, *Physics of Fluids*, Vol. 6, No. 10, pp. 3324-3334 (1994).